WEAKLY NONLINEAR ANALYSIS OF MULTIMODAL FLUVIAL BARS

Adichai PORNPROMMIN[1], Norihiro IZUMI[2] and Tetsuro TSUJIMOTO[3]

[1]Student Member of JSCE, Graduate Student, Dept. Civil Engineering, Nagoya University
(Furo-cho, Chikusa-ku, Nagoya 464-8603, Japan)
[2]Member of JSCE, Ph.D., Associate Professor, Dept. Civil Engineering, Tohoku University
[3]Member of JSCE, D.Eng., Professor, Dept. Geo-Environmental Engineering, Nagoya University

Fluvial bars are large-scale topography with a planimetric scale of the order of channel width, which appears on riverbeds when the aspect ratio is sufficiently large. In order to describe the formation of such multimodal fluvial bars, a weakly nonlinear analysis is performed in this paper with the use of the amplitude expansion method. In the analysis, the fundamental perturbations with four different harmonic modes are imposed on an initially flat riverbed. The equilibrium bar profiles obtained by the present multimodal analysis are comparable to those obtained from the uni-modal analysis and the numerical analysis when the aspect ratio is small. An irregularity in the time variation of bar amplitude that has not appeared in the uni-modal bar analysis, is promoted with increasing aspect ratio.

Key Words : *bar formation, multimodal nonlinear analysis, amplitude expansion method*

1. INTRODUCTION

Fluvial bars are large-scale topography with a planimetric scale of the order of channel width, which appears on riverbeds when the aspect ratio β (channel width/water depth) is sufficiently large. It is known that the bar formation is caused by the instability between flow and erodible beds, and that a flat bed becomes unstable and evolves into alternate bars or multiple bars.

The aspect ratio β is one of the most essential parameters for the bar formation. The alternate bar is the first unstable mode (m = 1) that appears just above the critical aspect ratio β_c. As β increases, the multiple bar (m > 1) starts to appear in river channels. It is known that regular patterns of multiple bars observed in the early stage of the experiments[1),2)] tend to transform into irregular patterns such as braided channels or self-formed low water channels.

Instability analyses of bars have been extensively performed for recent 40 years. At the beginning of the research, instability analyses were performed in term of linear level. Then, the focus has shifted to the nonlinear behavior of the finite amplitude bars beyond the linear region[3),4),5),6)]. The authors[6)] extended the analysis of Colombini *et al.*[4)] by employing the amplitude expansion method in order to investigate the equilibrium amplitudes of both alternate and multiple bars, and suggested that the multimodal interaction is one of the causes of irregularity that appears in the developing process. Fukuoka and Yamasaka[3)] performed a nonlinear analysis considering the interaction of two different modes, but they found no irregularity. Schielen *et al.*[5)] proposed another analysis to study more details of the instability of alternate bars. Considering perturbations growing in a narrow spectrum at near-critical aspect ratio β_c, they found a quasi-periodic behavior of the alternate bars.

In this study, we perform a weakly nonlinear analysis of bars considering the interaction between four different modes with the use of the amplitude expansion method in order to investigate the time development of bars.

2. FORMULATION

(1) Governing equations

Let us consider flow in a straight channel with a constant width W and non-erodible banks (Fig.1). The normalized St. Venant shallow water equations are expressed as

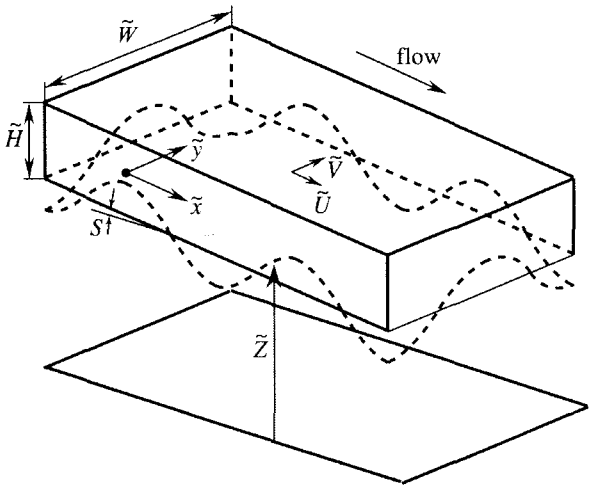

Fig.1 Sketch of coordinate system

$$F^2\left(U\frac{\partial U}{\partial x}+V\frac{\partial U}{\partial y}\right)= -\frac{\partial H}{\partial x}-\frac{\partial Z}{\partial x}-\beta S\frac{\left(U^2+V^2\right)^{1/2}U}{\left(1+2.5C_{fn}^{1/2}\ln H\right)^2 H} \tag{1}$$

$$F^2\left(U\frac{\partial V}{\partial x}+V\frac{\partial V}{\partial y}\right)= -\frac{\partial H}{\partial y}-\frac{\partial Z}{\partial y}-\beta S\frac{\left(U^2+V^2\right)^{1/2}V}{\left(1+2.5C_{fn}^{1/2}\ln H\right)^2 H} \tag{2}$$

$$\frac{\partial UH}{\partial x}+\frac{\partial VH}{\partial y}=0 \tag{3}$$

$$S=\frac{C_{fn}U_n^2}{gH_n},\quad F=\frac{U_n}{(gH_n)^{1/2}},\quad \beta=\frac{W}{H_n} \tag{4a-c}$$

where x and y are the streamwise and lateral coordinates respectively, U and V are the velocity components in the x and y directions respectively, H and Z are the flow depth and bed elevation respectively, S is the bed slope, F is the Froude number in the normal flow condition, β is the aspect ratio, and C_{fn}, U_n and H_n are the friction coefficient, streamwise velocity and flow depth in the normal flow condition, respectively.

The time variation of bed elevation can be described by the following normalized Exner sediment continuity equation:

$$\frac{\partial Z}{\partial t}+\frac{\partial Q_{bx}}{\partial x}+\frac{\partial Q_{by}}{\partial y}=0 \tag{5}$$

where t is time, and Q_{bx} and Q_{by} are the x and y components of the bedload transport rate. We use the linearized version of bedload formula by Kovacs and Parker[7], which includes the effects of local bed slope in the both streamwise and lateral directions. The normalized forms of the formula are

$$Q_{bx}=\left[\frac{U^2+V^2}{\left(1+2.5C_{fn}^{1/2}\ln H\right)^2}-\Theta-\frac{\Theta}{\mu_c\beta}\frac{\partial Z}{\partial x}\right] \times\left[\frac{\left(U^2+V^2\right)^{1/2}}{\left(1+2.5C_{fn}^{1/2}\ln H\right)}-\Theta^{1/2}-\frac{\Theta^{1/2}}{2\mu_c\beta}\frac{\partial Z}{\partial x}\right] /\left[\left(1+\frac{1}{\mu_c\beta}\frac{\partial Z}{\partial x}\right)(1-\Theta)\left(1-\Theta^{1/2}\right)\right] \tag{6}$$

$$Q_{by}=\left[\frac{U^2+V^2}{\left(1+2.5C_{fn}^{1/2}\ln H\right)^2}-\Theta\right] \times\left[\frac{\left(U^2+V^2\right)^{1/2}}{\left(1+2.5C_{fn}^{1/2}\ln H\right)}-\Theta^{1/2}\right] \times\left[\frac{V}{U}-\frac{\left(1+2.5C_{fn}^{1/2}\ln H\right)\Theta^{1/2}}{\left(U^2+V^2\right)^{1/2}\mu_c\beta}\frac{\partial Z}{\partial y}\right] /\left[(1-\Theta)\left(1-\Theta^{1/2}\right)\right] \tag{7}$$

where $\Theta=\tau_{co}/\tau_n$, τ_{co} is the critical Shields stress for a flat bed, and τ_n is the Shields stress in the normal flow condition.

The following normalization has been used to derive the above equations:

$$(\tilde{x},\tilde{y})=W(x,y),\quad (\tilde{U},\tilde{V})=U_n(U,V) \tag{8a-d}$$

$$(\tilde{H},\tilde{Z},\tilde{D}_s)=H_n(H,Z,D_s),\quad \tilde{t}=\frac{(1-\lambda_p)H_nB}{Q_n}t \tag{8e-h}$$

$$Q_n=(R_sg\tilde{D}_s^3)^{\frac{1}{2}}\frac{\alpha^{1/2}}{\mu_c}\left(\tau_n-\tau_{co}\right)\left(\tau_n^{1/2}-\tau_{co}^{1/2}\right) \tag{9}$$

where the tilde denotes the dimensional values, Q_n is the sediment transport rate in the normal flow condition, μ_c is the dynamic Coulomb friction factor, and α is the ratio of the shear velocity to the representative fluid velocity in the vicinity of the bed. Kovacs and Parker[7] suggested that $\mu_c = 0.84$ and $\alpha^{1/2} = 11.9$. These values are also used in this study.

(2) Multimodal asymptotic expansion

The following perturbation is imposed to the normal flow:

$$(U,V,H,Z)=(1,0,1,-\beta Sx)+(U_1,V_1,H_1,Z_1)+(U_2,V_2,H_2,Z_2) \tag{10}$$

where the subscript 1 and 2 denote the first order terms at $O(|A|,|B|,|C|,|D|)$ and the second order terms at $O(|A^2|,|B^2|,|C^2|,|D^2|)$, respectively. Assume that fundamental disturbances are expressed by small perturbations of four different modes m = 1, 2, 3 and 4 with small amplitudes (A, B, C and D), and their

wavenumbers are harmonics in the longitudinal direction described by m multiplied by k. The first order terms at $O(|A|,|B|,|C|,|D|)$ can be written as

$$\begin{aligned}(U_1,V_1,H_1,Z_1) &= AE_1\Gamma_1(u_{111},v_{111},h_{111},z_{111})+\text{c.c.}\\ &+BE_2\Gamma_2(u_{122},v_{122},h_{122},z_{122})+\text{c.c.}\\ &+CE_3\Gamma_3(u_{133},v_{133},h_{133},z_{133})+\text{c.c.}\\ &+DE_4\Gamma_4(u_{144},v_{144},h_{144},z_{144})+\text{c.c.}\end{aligned} \quad (11)$$

where c.c. denotes the complex conjugate of the preceding term, and E_m and Γ_m are

$$E_m = \exp m\mathbf{i}kx,\quad \Gamma_m = \begin{cases}\cos m\pi y & \text{for } U,H,Z\\ \sin m\pi y & \text{for } V\end{cases} \quad (12a,b)$$

In the second order, the nonlinearity by the interaction between the fundamental perturbations results in the deformation of the base flow with higher harmonics and lower harmonics both in the longitudinal and transverse directions. Since each of the fundamental perturbations has the factors $AE_1\Gamma_1$, $BE_2\Gamma_2$, $CE_3\Gamma_3$ and $DE_4\Gamma_4$, the interaction of the fundamental perturbations yields the second order terms with A^2, AA^*, B^2, BB^*, C^2, CC^*, D^2, DD^*, AB, A^*B, AC, A^*C, AD, A^*D, BC, B^*C, BD, B^*D, CD, C^*D as well as $E_i\Gamma_j$ (i,j = 0-8). Some examples of the terms produced by the nonlinear interaction can be described as

$$AE_1\Gamma_1 z_{111}\times AE_1\Gamma_1 z_{111} = A^2E_2\left(\Gamma_2 z_{222}^{AA}+z_{220}^{AA}\right) \quad (13a)$$

$$AE_1\Gamma_1 z_{111}\times A^*E_1^*\Gamma_1 z_{111}^* = AA^*\left(\Gamma_2 z_{202}^{AA^*}+z_{200}^{AA^*}\right) \quad (13b)$$

$$AE_1\Gamma_1 z_{111}\times BE_2\Gamma_2 z_{122} = ABE_3\left(\Gamma_3 z_{233}^{AB}+\Gamma_1 z_{231}^{AB}\right) \quad (13c)$$

where * denotes the complex conjugate.

The time development of the fundamental amplitudes can be described by the Landau equations. In this multimodal case, the development of the amplitudes is influenced by the nonlinear interaction with the second order terms, which possess the same harmonics as the fundamental perturbations $E_1\Gamma_1$, $E_2\Gamma_2$, $E_3\Gamma_3$, $E_4\Gamma_4$. As a result, the Landau equations take forms of the following four first-order differential equations with complex variables:

$$\frac{dA}{dt} = \lambda_0^A A+\lambda_1^A A^*B+\lambda_2^A B^*C+\lambda_3^A C^*D \quad (14)$$

$$\frac{dB}{dt} = \lambda_0^B B+\lambda_1^B A^2+\lambda_2^B A^*C+\lambda_3^B B^*D \quad (15)$$

$$\frac{dC}{dt} = \lambda_0^C C+\lambda_1^C AB+\lambda_2^C A^*D \quad (16)$$

$$\frac{dD}{dt} = \lambda_0^D D+\lambda_1^D AC+\lambda_2^D B^2 \quad (17)$$

where λ_0^j (j = A, B, C, D) are linear growth rates, λ_i^j (i = 1, 2, 3; j = A, B, C, D) are the Landau constants, and the terms with the orders higher than the second order are neglected. The above equations are easily solved numerically. We used the following initial conditions: $A(0) = 10^{-4}$, $B(0) = 10^{-5}$, $C(0) = 10^{-6}$, $D(0) = 10^{-7}$. It has been found that effects of initial conditions disappear after sufficiently long time as long as the initial values are sufficiently small.

(3) First order expansion

We have the following equations at the first order:

$$F^2\frac{\partial U_1}{\partial x}+\frac{\partial H_1}{\partial x}+\frac{\partial Z_1}{\partial x}+2\beta SU_1-\beta S\left(1+5C_{fn}^{\frac{1}{2}}\right)H_1 = 0 \quad (18)$$

$$F^2\frac{\partial V_1}{\partial x}+\frac{\partial H_1}{\partial y}+\frac{\partial Z_1}{\partial y}+\beta SV_1 = 0 \quad (19)$$

$$\frac{\partial U_1}{\partial x}+\frac{\partial H_1}{\partial x}+\frac{\partial V_1}{\partial y} = 0 \quad (20)$$

$$\frac{\partial Z_1}{\partial t}+\theta_{1,0}\frac{\partial U_1}{\partial x}+\frac{\partial V_1}{\partial y}-\frac{5}{2}C_{fn}^{1/2}\theta_{1,0}\frac{\partial H_1}{\partial x}-\frac{1}{2}\theta_{3,1}\frac{\partial^2 Z_1}{\partial x^2}-\theta_{2,1}\frac{\partial^2 Z_1}{\partial y^2} = 0 \quad (21)$$

where

$$\theta_{1,0} = \frac{3+\Theta^{1/2}}{1-\Theta},\ \theta_{2,1} = \frac{\Theta^{1/2}}{\mu_c\beta},\ \theta_{3,1} = \frac{2+\Theta^{1/2}+\Theta}{\mu_c\beta(1-\Theta)} \quad (22a\text{-}c)$$

By substituting the first order perturbations (11), the above equations are rewritten in matrix forms

$$\mathbf{L}_{abc}^{\phi}\begin{bmatrix}u_{abc}\\ v_{abc}\\ h_{abc}\\ z_{abc}\end{bmatrix} = 0,\quad a=1,\quad b=c=1,2,3,4 \quad (23a\text{-}d)$$

where the subscript a denotes the order of expansion, the subscripts b and c denote terms accompanying $E_b\Gamma_c$, and the superscript ϕ denotes terms with the amplitudes A, B, C, and D, respectively. The matrix $\mathbf{L}_{abc}^{\phi}$ can be written as

$$\mathbf{L}_{abc}^{\phi} = [l_{ij}],\quad i,j = 1,2,3,4 \quad (24a)$$

$$l_{11} = 2\beta S+\mathbf{i}bkF^2,\ l_{12} = 0,\ l_{13} = \mathbf{i}bk-\beta S\left(1+5C_{fn}^{1/2}\right),$$
$$l_{14} = \mathbf{i}bk,\ l_{21} = 0,\ l_{22} = \beta S+\mathbf{i}bkF^2,\ l_{23} = -c\pi,$$
$$l_{24} = -c\pi,\ l_{31} = \mathbf{i}bk,\ l_{32} = c\pi,\ l_{33} = \mathbf{i}bk,\ l_{34} = 0,$$
$$l_{41} = \mathbf{i}bk\theta_{1,0},\ l_{42} = c\pi,\ l_{43} = -5/2\left(\mathbf{i}bkC_{fn}^{1/2}\theta_{1,0}\right),$$
$$l_{44} = \Lambda_{abc}^{\phi}+\theta_{2,1}(c\pi)^2+\frac{1}{2}\theta_{3,1}(bk)^2 \quad (24b\text{-}q)$$

where

$$\Lambda_{111}^A = \lambda_0^A,\ \Lambda_{122}^B = \lambda_0^B,\ \Lambda_{133}^C = \lambda_0^C,\ \Lambda_{144}^D = \lambda_0^D \quad (25a\text{-}d)$$

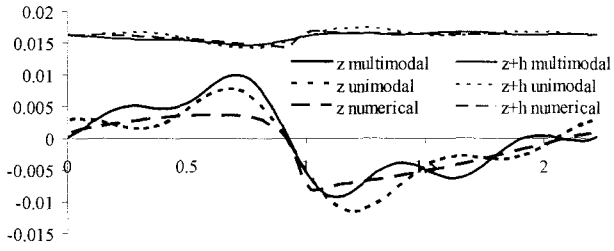

Fig.2 Longitudinal profiles by multimodal, unimodal and numerical simulation at $y = 1$ cm.

Fig.3 Bed topography for $\beta = 20$.

Solving (23*a-d*) with the solvability condition that the determinant of $\mathbf{L}^{\phi}_{1bc}$ must vanish for non-trivial solution, we can obtain the linear growth rates as functions of the parameters β, S, F, Θ and k.

(4) Second order expansion

We have the following equations at the second order:

$$F^2\frac{\partial U_2}{\partial x}+\frac{\partial H_2}{\partial x}+\frac{\partial Z_2}{\partial x}+2\beta S U_2-\beta S\left(1+5C_{fn}^{1/2}\right)H_2=P \tag{26}$$

$$F^2\frac{\partial V_2}{\partial x}+\frac{\partial H_2}{\partial y}+\frac{\partial Z_2}{\partial y}+\beta S V_2=Q \tag{27}$$

$$\frac{\partial U_2}{\partial x}+\frac{\partial H_2}{\partial x}+\frac{\partial V_2}{\partial y}=R \tag{28}$$

$$\frac{\partial Z_2}{\partial t}+\theta_{1,0}\frac{\partial U_2}{\partial x}+\frac{\partial V_2}{\partial y}-\frac{5}{2}C_{fn}^{1/2}\theta_{1,0}\frac{\partial H_2}{\partial x}-\frac{1}{2}\theta_{3,1}\frac{\partial^2 Z_2}{\partial x^2}-\theta_{2,1}\frac{\partial^2 Z_2}{\partial y^2}=S \tag{29}$$

where P, Q, R, and S on the right hand sides of (26)-(29) denote the inhomogeneous terms produced by the interaction of the fundamental perturbations (more details can be found in ref.6). Categorizing in terms of $E_i\Gamma_j$, P, Q, R, and S are separated into p_{2ij}, q_{2ij}, r_{2ij} and s_{2ij}, respectively (i, j = 0-8).

Since the nonhomogeneous heterogeneous terms include $E_i\Gamma_j$ (i, j = 0-8), the solutions of the second order expansion are expected to have the following form:

$$\left(U_2, V_2, H_2, Z_2\right)=\phi\sum_{b=1,c=1}^{8}\left(u^{\phi}_{2bc}, v^{\phi}_{2bc}, h^{\phi}_{2bc}, z^{\phi}_{2bc}\right)E_b\Gamma_c \tag{30}$$

where $\phi = A^2$, AA^*, B^2, BB^*, C^2, CC^*, D^2, DD^*, AB, A^*B, AC, A^*C, AD, A^*D, BC, B^*C, BD, B^*D, CD, C^*D.

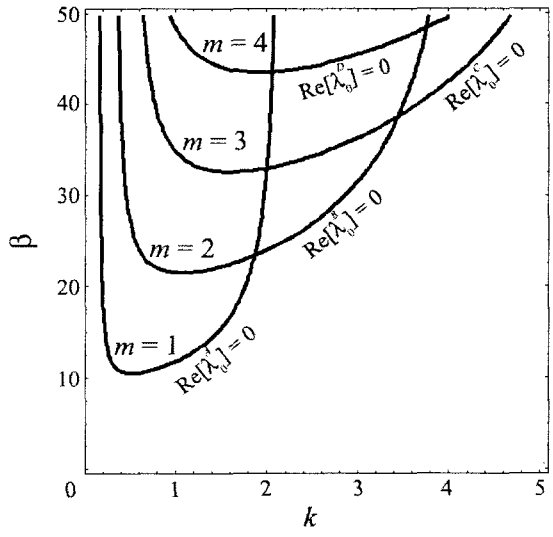

Fig.4 Instability curves. (Flat beds are unstable in the region enclosed by curves.)

By substituting (30), (26)-(29) are rewritten in the following matrix forms

$$\mathbf{L}^{\phi}_{abc}\begin{bmatrix}u^{\phi}_{abc}\\ v^{\phi}_{abc}\\ h^{\phi}_{abc}\\ z^{\phi}_{abc}\end{bmatrix}=\begin{bmatrix}p^{\phi}_{abc}\\ q^{\phi}_{abc}\\ r^{\phi}_{abc}\\ s^{\phi}_{abc}-z_{1bc}\lambda_i^j\end{bmatrix},\ a=2,\ b=c=1,2,3,4 \tag{31a-j}$$

where λ_i^j are the Landau constants, (ϕ, i, j) are (A^*B, 1, A), (B^*C, 2, A), (C^*D, 3, A), (AA, 1, B), (A^*C, 2, B), (B^*D, 3, B), (AB, 1, C), (A^*D, 2, C), (AC, 1, D) and (BB, 2, D). The matrix $\mathbf{L}^{\phi}_{2bc}$ can be obtained from (24*a-q*) with a replaced by 2, and the term Λ^{ϕ}_{2bc} in $\mathbf{L}^{\phi}_{2bc}$ are expressed as

$$\begin{aligned}
&\Lambda^{A^*B}_{211}=\left(\lambda_0^A\right)^*+\lambda_0^B,\quad \Lambda^{B^*C}_{211}=\left(\lambda_0^B\right)^*+\lambda_0^C,\\
&\Lambda^{C^*D}_{211}=\left(\lambda_0^C\right)^*+\lambda_0^D,\quad \Lambda^{AA}_{222}=2\lambda_0^A,\\
&\Lambda^{A^*C}_{222}=\left(\lambda_0^A\right)^*+\lambda_0^C,\quad \Lambda^{B^*D}_{222}=\left(\lambda_0^B\right)^*+\lambda_0^D,\\
&\Lambda^{AB}_{233}=\lambda_0^A+\lambda_0^B,\quad \Lambda^{A^*D}_{233}=\left(\lambda_0^A\right)^*+\lambda_0^D,\\
&\Lambda^{AC}_{244}=\lambda_0^A+\lambda_0^C,\quad \Lambda^{BB}_{244}=2\lambda_0^B
\end{aligned} \tag{32a-j}$$

The Landau constants in the second order cannot be determined uniquely from the above equations. This was a critical problem with the amplitude expansion method. Herbert[8] resolved this problem by introducing a clear definition of the amplitude. Therefore, the amplitudes of the fundamentals with the factors $E_1\Gamma_1$, $E_2\Gamma_2$, $E_3\Gamma_3$ and $E_4\Gamma_4$ are redefined as A, B, C and D, respectively. The following normalization is then possible:

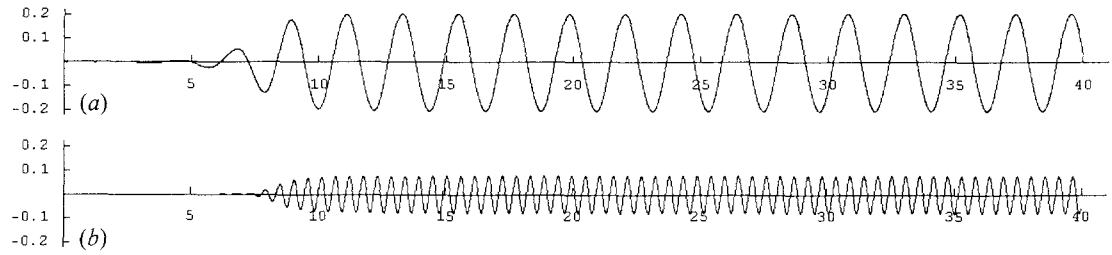

Fig.5 Time development of the fundament amplitudes for $\beta = 20$; (*a*) Re[*A*] and (*b*) Re[*D*].

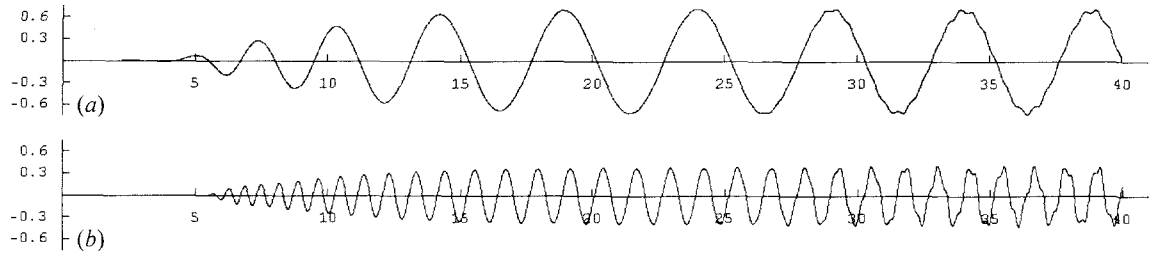

Fig.6 Time development of the fundament amplitudes for $\beta = 25$; (*a*) Re[*A*] and (*b*) Re[*D*].

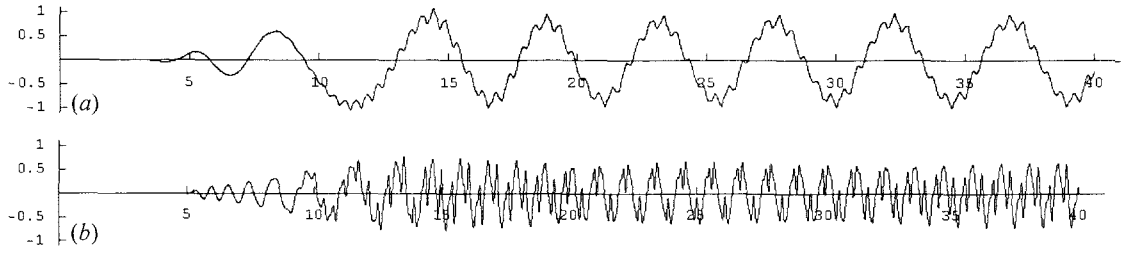

Fig.7 Time development of the fundament amplitudes for $\beta = 27.5$; (*a*) Re[*A*] and (*b*) Re[*D*].

$$z_{1ii} = 1, \quad z_{2ii} = 0, \quad i = 1, 2, 3, 4 \tag{33}$$

Solving the matrices (31*a-j*) with the use of the normalization by (33) provides the Landau constants in the second order.

3. RESULTS AND DISCUSSION

The Landau constants both in the linear and nonlinear levels can be computed by substituting the non-dimensional parameters as follows:

$$\lambda_i^j = f_i^j(\beta, S, F, \Theta, k),\ i = 0\text{-}3 \text{ and } j = A, B, C, D \tag{34}$$

From the experiments by Ikeda[9], Run No.18 is taken up in order to investigate the behavior of bar development. Dimensional hydraulic parameters applied in the experiment are transformed into non-dimensional parameters: $\beta = 20$, $S = 0.0104$, $F = 1.07$, $\Theta = 0.508$ and $k = 0.9$.

A comparison among the multimodal analysis, the uni-modal analysis[6] and the numerical simulation[10] is shown in Fig.2. The profile of the multimodal analysis is obtained by substituting the amplitudes from *A* to *D* calculated by (14)-(17) into (11) while the uni-modal analysis is performed up to the third order because our main objective is to investigate the qualitative features of the multimodal bar interaction. Nevertheless, we found that the profile obtained in the multimodal analysis is comparable with those of the other analyses. The equilibrium bar height obtained in the experiment, the multimodal analysis, the uni-modal analysis and the numerical simulation are 2.25, 1.25, 1.67 and 1.24 cm, respectively. Figure 3 shows the contours of bed topography computed in the present analysis, where a brighter color corresponds to a higher elevation.

Let us study the behavior of bar amplitude when the aspect ratio increases. The instability diagram for four different modes $m = 1$, 2, 3 and 4 obtained from the uni-modal analysis is shown in Fig.4. Figures 5*a* and 5*b* show the time variations of the real parts of the amplitudes *A* and *D*, respectively, in the case $\beta = 20$, in which the mode $m = 1$ is in unstable regime and the other modes $m = 2$, 3, and 4 are in stable regime. Though *B* and *C* are omitted because of the limitation of space, they show rather regularly periodic patterns as well as *A* and *D*. It is found that, even though the modes $m = 2$, 3 and 4 are in stable regime, they are excited to be unstable

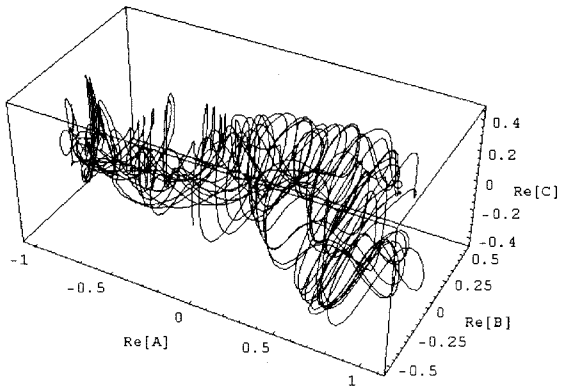

Fig.8 Parametric plot of Re[A], Re[B] and Re[C] for $\beta = 27.5$.

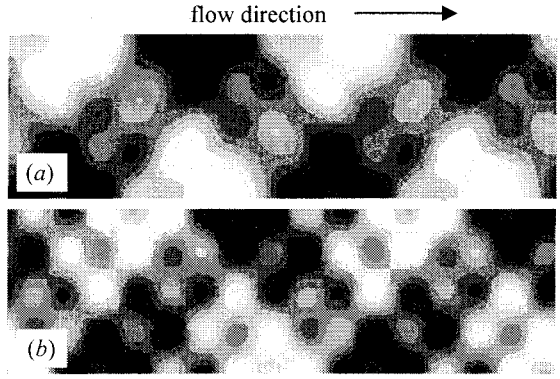

Fig.9 Bed topographies for $\beta = 27.5$; (a) $t = 40$ and (b) $t = 100$.

due to the multimodal interaction.

The results in the case $\beta = 25$ are shown in Fig.6. In comparison with Fig.5, the average amplitude increases with the aspect ratio β. It is found that small fluctuations are superposed on the regular oscillation due to the multimodal interaction.

Figure 7 shows the results in the case $\beta = 27.5$. The time development of the bar amplitude is shown to become more irregular. Figure 8 shows the parametric plot of the real parts of the amplitudes A, B and C from $t = 0$ to $t = 40$. The three-dimensional position of each point represents the values of A, B and C at a certain instant. The path shows a complex pattern, which implies the irregularity of the time variation of bed topography. Remind that we focus on the irregularity in the time variation of bar amplitude, so that the spatial distribution of bar amplitude never becomes irregular in the analysis.

Examples of the contour to express bed topography for the case $\beta = 27.5$ is shown in Fig.9. It is found that bed topography deforms itself because of the fluctuations as time developed.

It is known that the regular patterns of multiple bars are unstable and are easily evolved into complex braided patterns characterized by the chaotic behavior[1]. This analysis suggests that the irregularity in time variation can be produced by the multimodal interaction of the first four simplest unstable modes (m = 1, 2, 3 and 4) when the aspect ratio is high. If more modes are included in the analysis, the irregularity is expected to be emphasized. However, it should be noted that it has not been clarified if the irregularity shown in this analysis has the same chaotic features as real braided patterns have. This needs further study.

4. CONCLUSION

A multimodal analysis of four different modes m =1, 2, 3 and 4 is performed with the use of the amplitude expansion method. The major results obtained from the analysis are the following:

- An equilibrium bar profile obtained from the present analysis is found to be comparable to those obtained from the uni-modal analysis and the numerical simulation, even though only the lower order terms are taken into account.
- The multimodal interaction causes the irregularity in the time variation of the bar amplitudes. The irregularity is promoted with increasing aspect ratio.

REFERENCES

1) Fujita, Y.: Bar and channel formation in braided streams, *River meandering*, S. Ikeda and G. Parker, eds., Water Resource Monograph, Vol. 12, AGU, pp.417-462, 1989.
2) Takebayashi, H., Egashira, S. and Okabe, T.: Stream formation process between confining banks of straight wide channels, 2nd *Proc. RCEM*, IAHR, Japan, pp.575-584, 2001.
3) Fukuoka, S. and Yamasaka, M.: Equilibrium height of alternate bars based on non-linear relationships among bed profile, flow and sediment discharge, *Proc. of JSCE*, Vol. 357/II-3, pp.45-54, 1985. (in Japanese)
4) Colombini, M., Seminara, G. and Tubino, M.: Finite amplitude alternate bars, *J. Fluid Mech.*, Vol. 181, pp.213-232, 1987.
5) Schielen, R., Doelman, A. and de Swart, H. E.: On the nonlinear dynamics of free bars in straight channels, *J. Fluid Mech.*, Vol. 252, pp.325-356, 1993.
6) Izumi, N. and Pornprommin, A.: Weakly nonlinear analysis of bars with the use of the amplitude expansion method, *J. Hyd., Coastal and Env. Eng.*, No. 712/II-60, JSCE, pp.73-86, 2002. (in Japanese)
7) Kovacs, A. and Parker, G.: A new vectorial bedload formulation and its application to the time evolution of straight channels, *J. Fluid Mech.*, Vol.267, pp.153-183, 1994.
8) Herbert, T.: On perturbation methods in nonlinear stability theory, *J. Fluid Mech.*, Vol.126, pp.167-186, 1983.
9) Ikeda, S.: Prediction of alternate bar wavelength and height, *J. Hydrau. Eng.*, Vol.110(4), ASCE, pp.371-386, 1984.
10) Pornprommin, A., Teramoto, A., Izumi, N., Kitamura, T. and Tsujimoto, T.: Numerical simulation of bar formation in straight channels by the NHSED2D model, *J. Applied Mech.*, Vol.5, JSCE, pp.629-638, 2002.

(Received September 30, 2003)